ECE 796:

Models of the Neuron

Slides for Lecture #7

Monday, March 2, 2009

Rinzel and Ermentrout (1998)

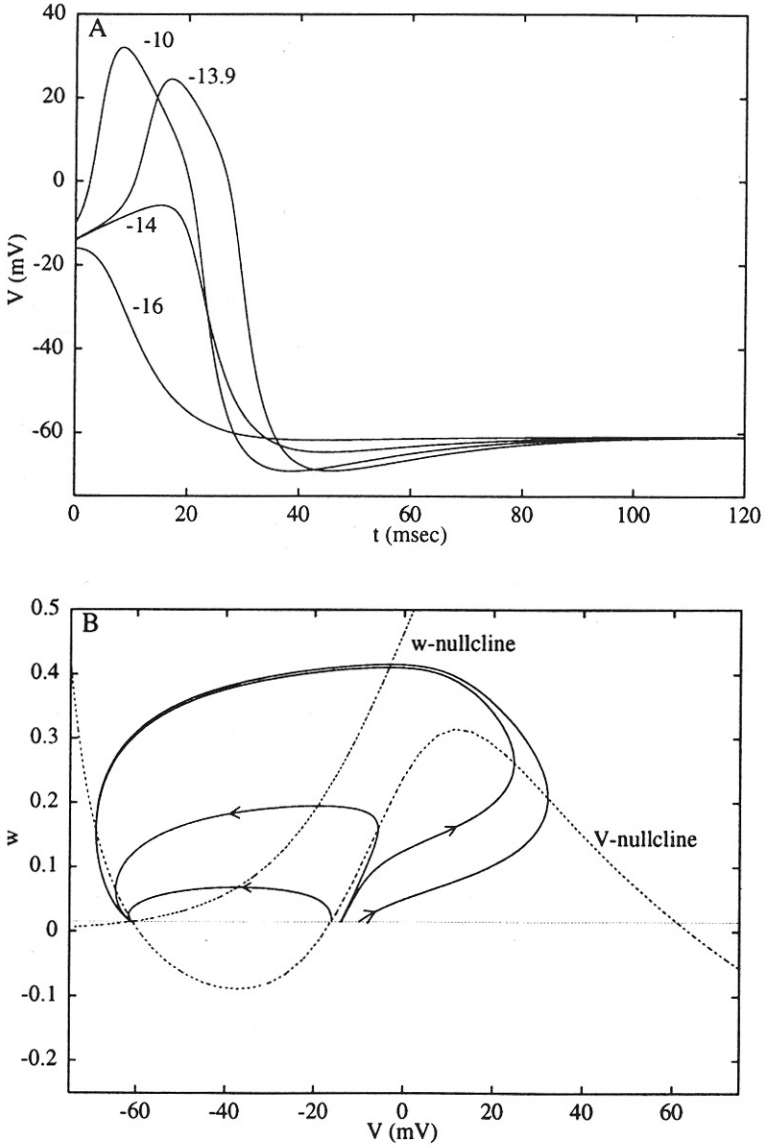

Figure 7.1
Response of the Morris-Lecar excitable system, eqs. 7.4–7.6, to a brief current pulse. For these parameters (see appendix A), the system has a unique stable rest state, $\bar{V} = -61\,\text{mV}$, $\bar{w} = .015$. The line $w = \bar{w}$ is shown lightly dashed. Four different stimuli lead to an instantaneous displacement of V from $\bar{V}$ to V_0 (values of V_0 are shown alongside the curves in panel A). Panel A shows the time course of the voltage. Notice that intermediate responses are possible with some stimuli: the threshold is graded; firing occurs with finite latency. Panel B shows trajectories in the V-w phase plane; nullclines are shown dashed and intersect only once. The effect of a stimulus is to displace the initial condition horizontally from rest.

Rinzel and Ermentrout (1998)

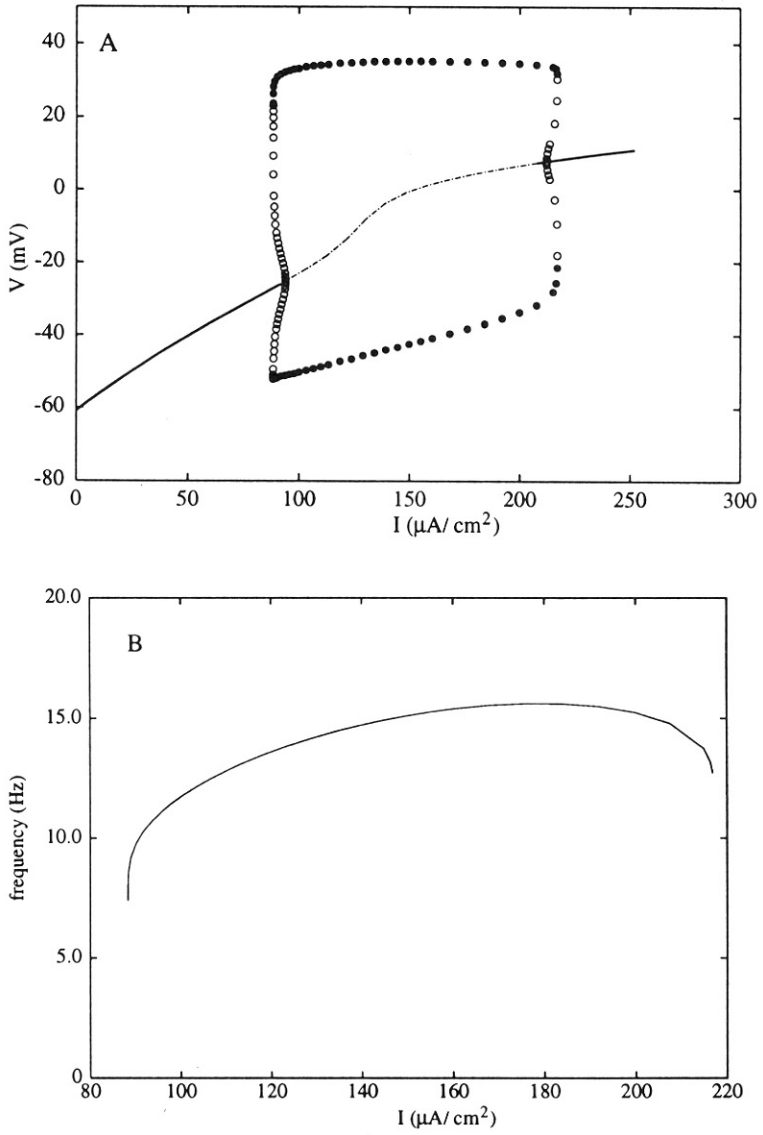

Figure 7.2
Repetitive firing in the Morris-Lecar model for steady current. Bifurcation diagram in panel A shows the steady-state voltage $\bar{V}$ versus I (thin lines; stable are solid, unstable are dashed) and the maximum and minimum voltage for periodic solutions shown as filled (stable) and unfilled (unstable) circles. The unstable branch of periodic solutions meets the branch of steady-state oscillations at $I = I_1 = 94\,\mu A/cm^2$ and $I = I_2 = 212\,\mu A/cm^2$ (Hopf bifurcation points). The unstable branch of periodic solutions coalesces with the stable branch of periodic solutions at $I = I_v = 88\,\mu A/cm^2$. A similar coalescence occurs near $I = 215\,\mu A/cm^2$. For these parameters, the steady-state I-V curve is monotonic. Furthermore, panel B shows that the frequency (plotted in Hz, and only for the stable limit cycles) as a function of current is always bounded away from zero. Parameters are as figure 7.1.

Rinzel and Ermentrout (1998)

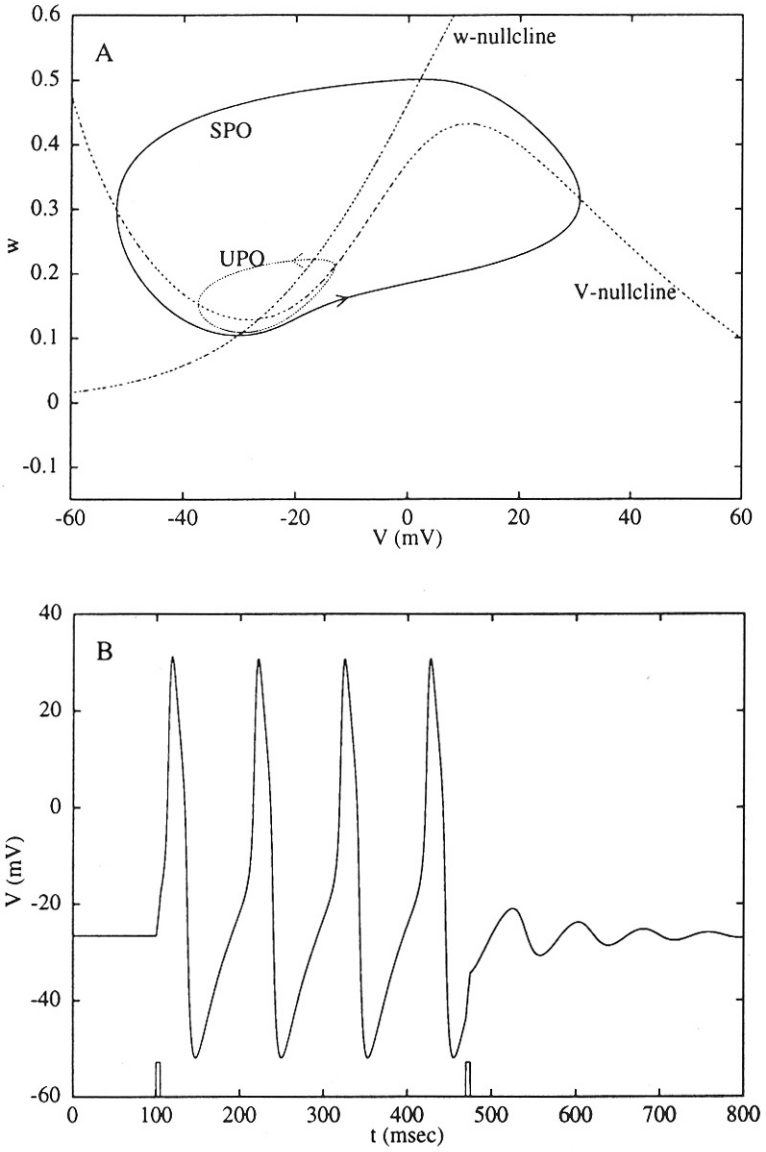

Figure 7.3
Bistability for steady current near the threshold for repetitive firing for the Morris-Lecar model with parameters as in figure 7.1 and $I = 90\,\mu A/cm^2$. In this region, where I is between the first Hopf bifurcation point, I_1, and the "knee," I_v, there are two stable states (cf figure 7.2): a rest state (the intersection of the nullclines) and a stable oscillation (SPO) separated by an unstable periodic solution (UPO). This is shown in panel A. Panel B demonstrate switching from rest to oscillation and then back to rest for two brief appropriately timed depolarizing current pulses.

Rinzel and Ermentrout (1998)

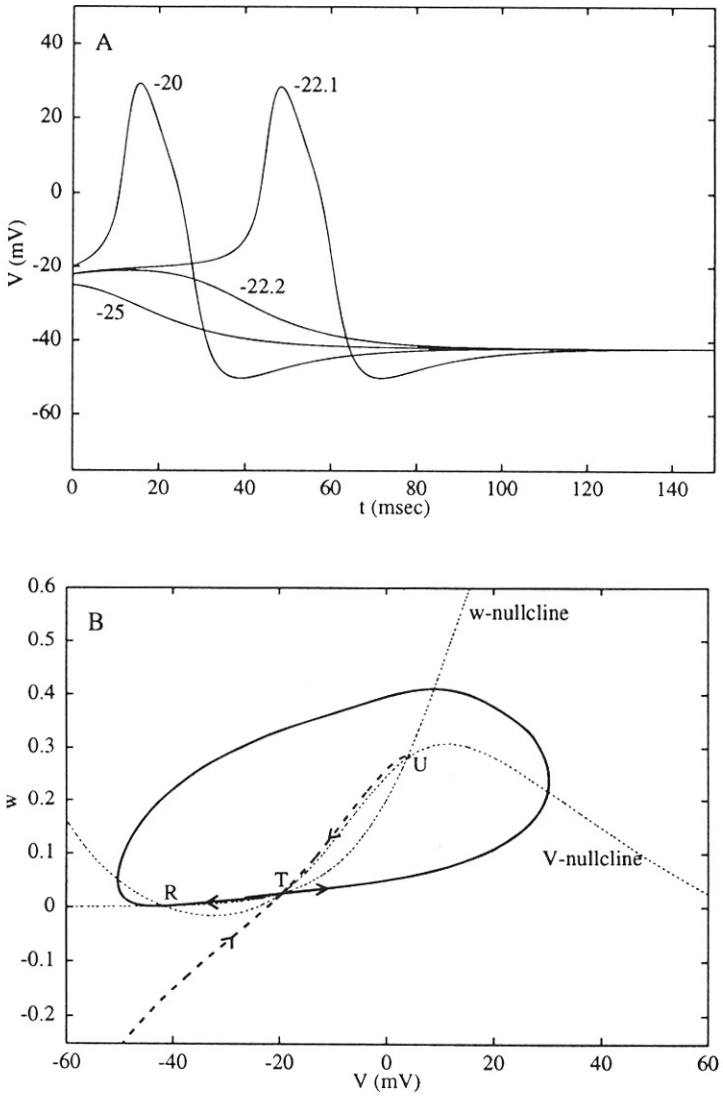

Figure 7.4
Excitability with three steady states and a distinct threshold; the response of the membrane to a brief current pulse from the stable rest state. Four different stimuli result in a displacement of V from $\bar{V}$ to V_0 (values of V_0 are given alongside the curves in panel A). (A) Time course of the voltage for $I = 30\,\mu A/cm^2$. (B) Phase plane for the dynamics illustrated in panel A. Nullclines intersect at three places: (1) R a stable rest state, (2) T, a saddle point threshold, and (3) U an unstable node. The thick solid line shows the unstable manifold for the saddle point; here, unstable refers to movement in opposing directions away from T (indicated by arrowheads). The manifold's two branches lead to the stable rest state and form a smooth loop in phase space. The heavy dashed line shows the stable manifold for the saddle point (arrowheads pointing toward T). Any initial conditions to the left of this manifold decay to rest. Initial conditions to the right lead to an action potential before returning to rest. Parameters are as in figure 7.1, except $\bar{g}_{Ca} = 4\,mS/cm^2$, $V_3 = 12\,mV$, $V_4 = 17.4\,mV$, $\phi = 1/15$.

Rinzel and Ermentrout (1998)

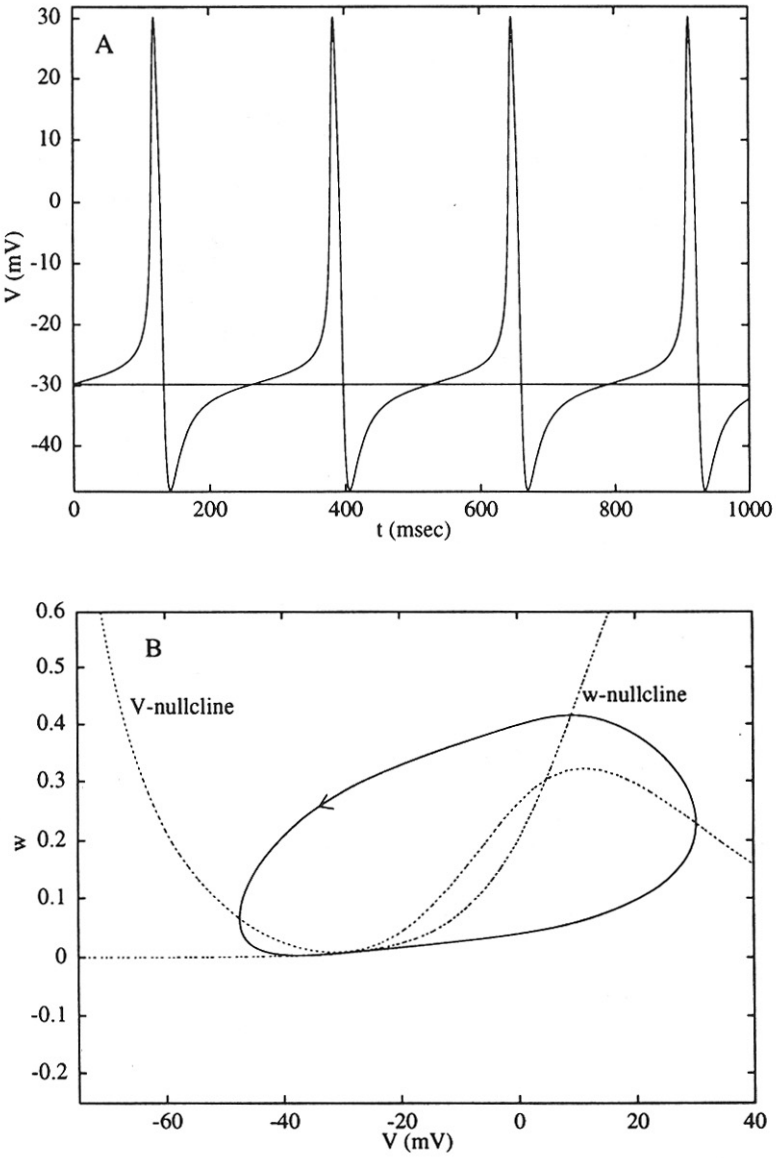

Figure 7.5
Onset of repetitive firing with arbitrarily low frequency for a constant current, $I = 40.76\,\mu A/cm^2$ shows an oscillation with a period of about 220 msec. Panel A shows the voltage time course and panel B shows the phase plane. Note the "narrow channel" between the two nullclines near $-30\,mV$, which accounts for most of the oscillation period (see Rinzel and Ermentrout 1989). Parameters are as in figure 7.4.

Rinzel and Ermentrout (1998)

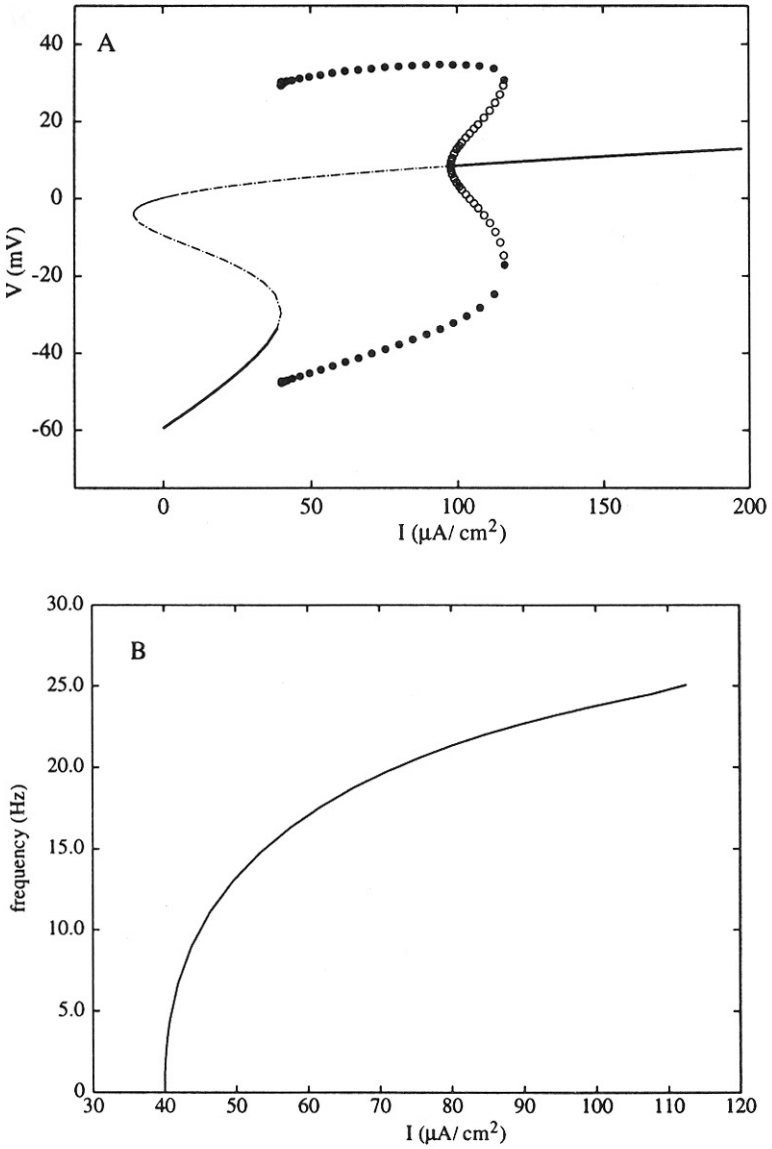

Figure 7.6
Multiple steady states and periodic orbits for a steady current when the I_{ss}–V relation is N-shaped. (A) Bifurcation diagram (line types as in figure 7.2A; parameters are as in figures 7.4–7.5). In spite of the coexistent states, the system is monostable for I between $I_1 = 40$, the turning point of the steady states, and $I_2 = 98$ where there is a Hopf bifurcation. Onset of repetitive firing at zero frequency occurs at $I = I_1$ where two fixed points coalesce. This corresponds to figure 7.4B when the unstable manifolds of the saddle point form a closed loop. The branch of periodic orbits has a turning point at $I = 116$ before terminating at the Hopf bifurcation point, $I = I_2$. All current values in $\mu A/cm^2$. (B) Frequency (in Hz) of stable branch of periodic orbits.

Rinzel and Ermentrout (1998)

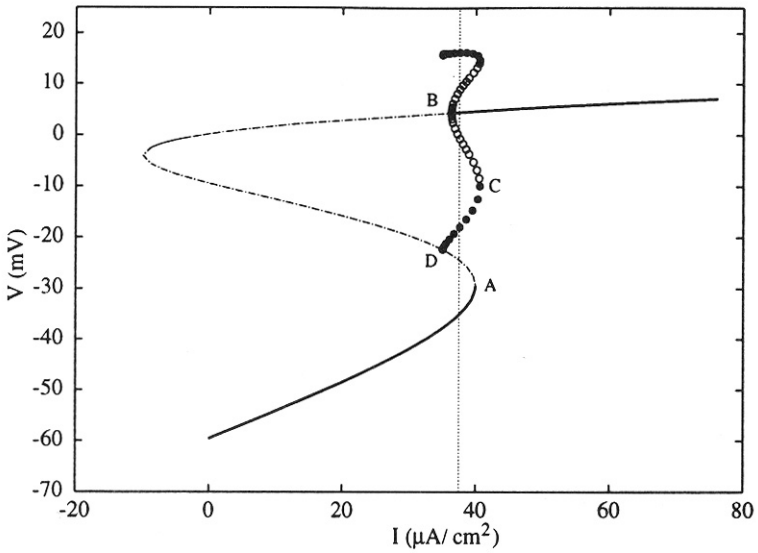

Figure 7.7
Bifurcation diagram (as in figure 7.6 but for $\phi = 0.23$). Point A shows where the two lower steady states coalesce, point B shows the Hopf bifurcation for the upper steady state, point C shows the coalescence of the stable and unstable periodic branches, and point D shows where the branch of stable oscillatory solutions terminates on the branch of saddle points (not on the knee, as in figure 7.6) at a saddle loop homoclinic. For currents between points B and A, there are three stable states: (1) a low-voltage rest state, (2) a high-voltage rest state, and (3) an oscillatory state. Note that the steady-state branch is identical to that of figure 7.6; ϕ only affects the stability of the steady states and the behavior of the periodic orbits. Vertical line at $I = 37.5\,\mu A/cm^2$ shows a current for which there are three stable states (cf. figure 7.8).

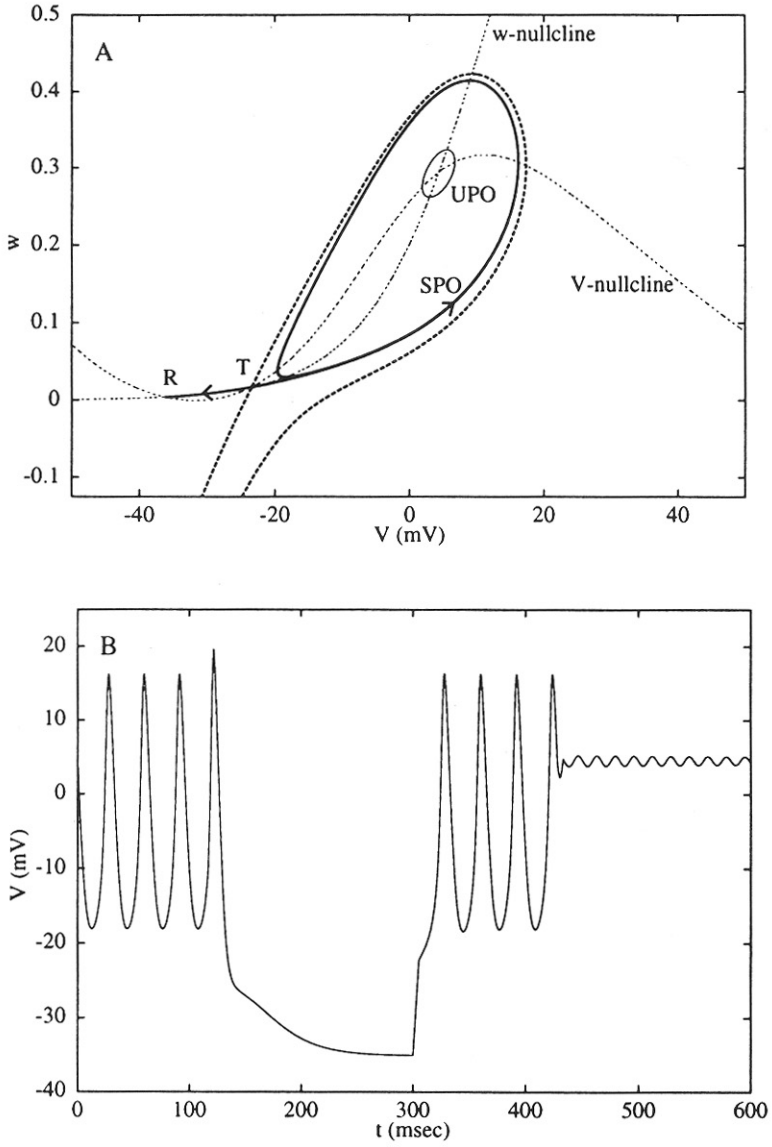

Figure 7.8
Multistability for a current between points B and A in figure 7.7 ($I = 37.5\,\mu A/cm^2$; other parameters are as in figure 7.7). Panel A depicts the V-w phase plane. The nullclines intersect at three places representing steady states: (1) a lower stable rest state (R), (2) an unstable saddle point (T), and (3) an upper stable rest state (unlabeled). The left branch of the unstable manifold of the saddle point (bold line) connects to the lower steady state. The right branch wraps around the stable periodic orbit (SPO). The branches of the stable manifold of the saddle point (bold dashed line) form a separatrix between the lower stable rest state and the stable periodic orbit. The unstable periodic orbit (UPO) separates the stable upper steady state from the stable periodic orbit. Panel B shows the effects of three successive depolarizing current pulses. Starting on the stable oscillation, the membrane is switched to the lower stable steady state. Another brief pulse pushes it back to the stable oscillation and a third pulse switches it to the upper steady state. No single brief current pulse can switch it from the lower steady state directly to the upper steady state, although the opposite transition is possible.

Rinzel and Ermentrout (1998)

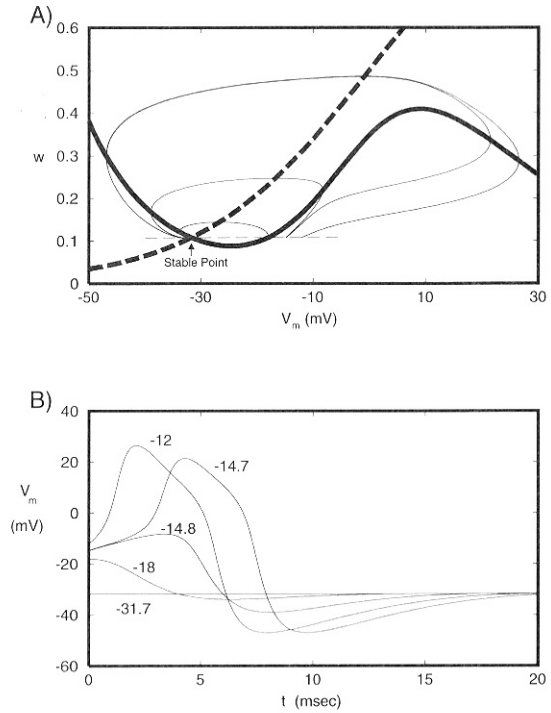

Fig. 7.7 Response of the Morris–Lecar Model to Current Pulses Equations 7.11, describing electrical events in the muscle cells of barnacles (Morris and Lecar, 1981), show a qualitatively similar behavior to the squid axon membrane and to the FitzHugh–Nagumo equations. **(A)** Phase plane portrait (here membrane potential V_m versus potassium activation w) for different stimulus conditions. The nullclines are plotted in bold. In the presence of a stabilizing current injection, the resting potential is -31.7 mV. From this state, the system is stimulated by brief current pulses, instantly depolarizing the membrane (thin lines). If the stimulus depolarizes the muscle to either -18 or to -14.8 mV, the system responds with a subthreshold excursion around the resting potential (two innermost loops around the resting potential). For larger values, the system moves along a limit cycle: it spikes. **(B)** Evolution of the membrane potential V_m for this stimulus paradigm.

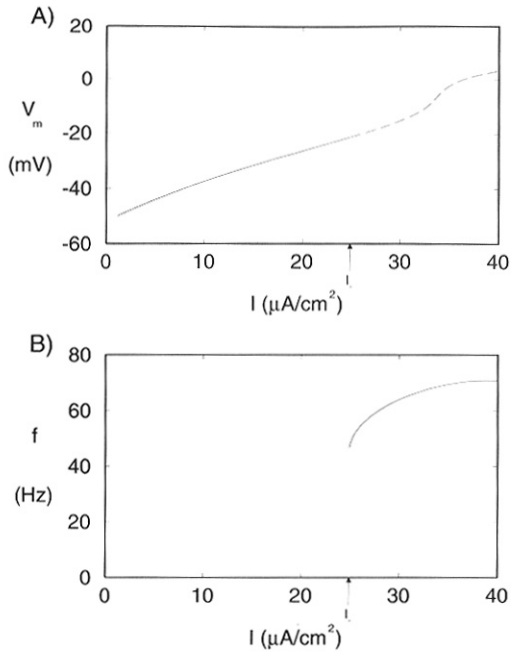

Fig. 7.8 Sustained Spiking in the Morris–Lecar Model **(A)** Steady-state voltage and **(B)** oscillation frequency as a function of the amplitude of the sustained current I for the reduced Morris–Lecar model (Eqs. 7.11). The steady-state I–V curve can also be viewed as the cumultative, steady-state ionic current flowing at any particular membrane potential V_m. At $I_{-} = 24.9\ \mu\text{A/cm}^2$ (arrow), the single equilibrium point (Fig. 7.7A) loses stability via hard excitation (a subcritical Hopf bifurcation) when the real part of the two conjugate eigenvalues goes through zero and becomes positive. As in the case for the Hodgkin–Huxley and FitzHugh–Nagumo equations, this type of onset of oscillations implies a nonzero oscillation frequency (here a minimum of 50 Hz).

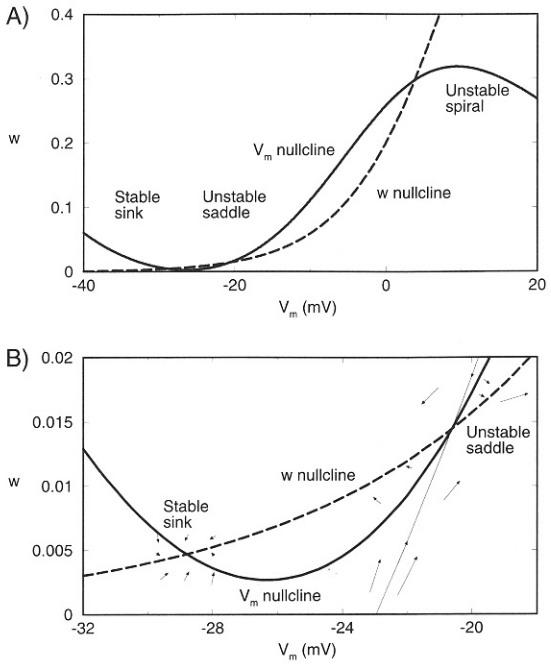

Fig. 7.9 System with Multiple Equilibrium Points The Morris–Lecar equations were modified by changing the dynamics of potassium activation and making its voltage dependency steeper (Eqs. 7.16 and 7.17). **(A)** Under these conditions, the two nullclines can intersect up to three times. Here, the lower equilibrium point is a globally attracting, *stable sink*, the middle one an *unstable saddle*, and the upper one an *unstable spiral*. **(B)** Phase space portrait around the two lower equilibrium points. The separatrix curve (thin line) at the saddle strictly separates sub- and suprathreshold regions of phase space. Points to the left of this curve will decay back to the stable sink, while points to the right will lead to a spike. If the current injected into the system is further increased, these two equilibrium points will move toward each other, coalesce, and disappear. If the initial state of the system lies in the neighborhood of these two curves, it will evolve very slowly since, by definition, $\dot{V}_m = 0$ along the V_m nullcline and $\dot{w} = 0$ along the w nullcline, explaining why the system is able to spike at very low frequencies.

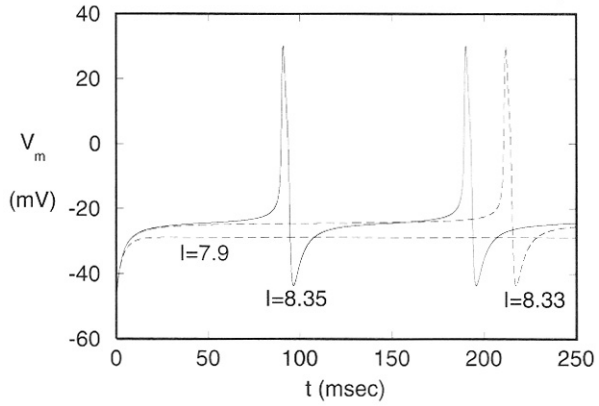

Fig. 7.10 SPIKING AT LOW FREQUENCIES Response of the modified Morris–Lecar equations (Eqs. 7.16 and 7.17) using current steps (starting at $t = 0$) of variable amplitude. In response to a current step of 7.9 μA/cm^2 amplitude, the membrane depolarizes. Close to $I_1 = 8.326$ μA/cm^2, the onset of spiking can be delayed almost indefinitely, similar to the delay observed in pyramidal cells due to the presence of the A-like current (Fig. 9.7). This is not caused by the very slow time constant of any one ionic current, but it is due to the structure of the nullclines in phase space (Fig. 7.9B).

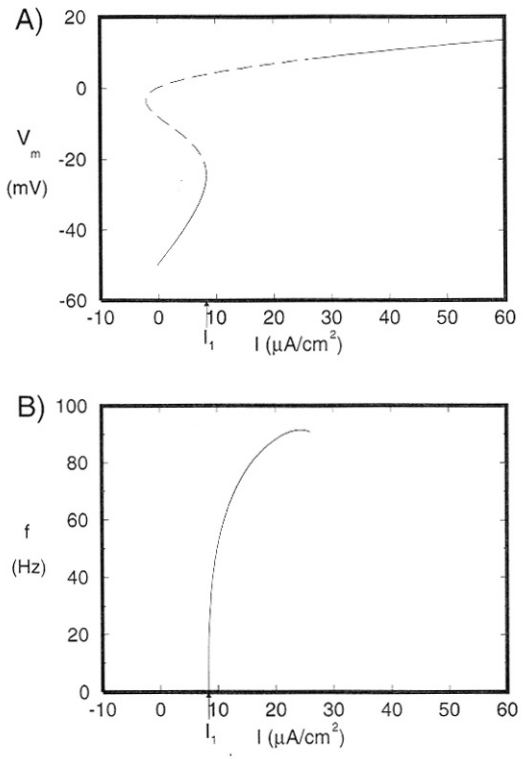

Fig. 7.11 Sustained Spiking in the Modified Morris–Lecar Model (A) Steady-state voltage and **(B)** oscillation frequency as a function of I for the modified Morris–Lecar model (Eqs. 7.16 and 7.17). Different from Fig. 7.8, the I–V relationship is N–shaped. Spiking first occurs at I_1 (arrow) when the slope of this curve is infinite and then becomes negative. This happens when the two lower equilibrium points in the phase portrait of Fig. 7.9 merge, creating oscillations with arbitrarily long interspike intervals via a saddle-node bifurcation.